BIOCHEMICAL PHARMACOLOGY 74 (2007) 831–840

available at www.sciencedirect.com

ScienceDirect

journal homepage: www.elsevier.com/locate/biochempharm

Inhibition of bacterial cell division protein FtsZ by cinnamaldehyde

Prerna Domadia [a,1], *Sanjay Swarup* [b,2], *Anirban Bhunia* [c,2], *J. Sivaraman* [b,**], *Debjani Dasgupta* [a,*]

[a] *Department of Biochemistry, The Institute of Science, Mumbai 400032, India*
[b] *Department of Biological Sciences, National University of Singapore, Singapore*
[c] *School of Biological Sciences, Nanyang Technological University, Singapore*

ARTICLE INFO

Article history:
Received 20 April 2007
Accepted 11 June 2007

Keywords:
Cinnamaldehyde
Z-ring
FtsZ
Polymerization
GTPase
Cell division

ABSTRACT

Cinnamaldehyde is a natural product from spices that inhibits cell separation in *Bacillus cereus*. Cell division is regulated by FtsZ, a prokaryotic homolog of tubulin. FtsZ assembles into the Z-ring at the site of cell division. Here, we report the effect of cinnamaldehyde on FtsZ and hence on the cell division apparatus. Cinnamaldehyde decreases the *in vitro* assembly reaction and bundling of FtsZ. It is found that cinnamaldehyde perturbs the Z-ring morphology *in vivo* and reduces the frequency of the Z ring per unit cell length of *Escherichia coli*. In addition, GTP dependent FtsZ polymerization is inhibited by cinnamaldehyde. Cinnamaldehyde inhibits the rate of GTP hydrolysis and binds FtsZ with an affinity constant of $1.0 \pm 0.2\ \mu M^{-1}$. Isothermal titration calorimetry reveals that binding of cinnamaldehyde to FtsZ is driven by favorable enthalpic interactions. Further, we map the cinnamaldehyde binding region of FtsZ, using the saturation transfer difference–nuclear magnetic resonance and an *in silico* docking model. Both predict the cinnamaldehyde binding pocket at the C terminal region involving the T7 loop of FtsZ. Our results show that cinnamaldehyde binds FtsZ, perturbs the cytokinetic Z-ring formation and inhibits its assembly dynamics. This suggests that cinnamaldehyde, a small molecule of plant origin, is a potential lead compound that can be developed as an anti-FtsZ agent towards drug design.

* *Corresponding author at*: Department of Biochemistry, The Institute of Science, 15 Madam Cama Road, Mumbai 400032, India. Tel.: +91 22 22844219x501.
** *Corresponding author at*: Department of Biological Sciences, National University of Singapore, Singapore 117543, Singapore. Tel.: +65 6516 1163.
E-mail addresses: dbsjayar@nus.edu.sg (J. Sivaraman), drdasgupta88@rediffmail.com (D. Dasgupta).
[1] Present address: School of Biological Sciences, Nanyang Technological University, Singapore.
[2] Both authors contributed equally.

Abbreviations: FtsZ, filamentation temperature sensitive protein Z; GTP, guanosine 5-triphosphate; MES, 2-morpholinoethanesulfonic acid; GFP, green fluorescent protein; STD NMR, saturation transfer difference–nuclear magnetic resonance; MIC, minimum inhibitory concentration; MBC, minimum bactericidal concentration; MRSA, methicillin resistant *Staphylococcus aureus*; FPLC, fast protein liquid chromatography; ITC, isothermal titration calorimetry; T7, tubulin like loop 7; LB, Luria-Bertani; DMSO, dimethyl sulfoxide

0006-2952/$ – see front matter
doi:10.1016/j.bcp.2007.06.029

1. Introduction

FtsZ, a 40-kDa protein is a highly promising target for new antibacterial drugs because of its central role in bacterial cell division [1]. FtsZ undergoes GTP-dependent polymerization into filaments, which assemble into a highly dynamic polymeric structure known as the Z-ring on the inner membrane of the mid-cell [2]. FtsZ is an attractive drug target due to its widespread conservation in the bacterial kingdom, its absence in the mitochondria of higher eukaryotes and its evolutionary distance from eukaryotic tubulin [3]. Recently, a number of FtsZ inhibitors have been reported. Of the known *E. coli* FtsZ inhibitors, viriditoxin [4], dichamantin [5], 2-hydroxy-5-benzylisouvarinol-B [5], 2,4,6-trihydroxy-3,5-di(2′-hydroxybenzyl)-acetophenone [5] do seem to inhibit Gram-positive bacteria, whereas zantrins Z1-Z5 [6], sanguinarine [7] and A189 [8] are potent inhibitors of broad range of pathogenic bacteria. Z5 [6] and A189 [8] perturb the FtsZ ring assembly with the inhibition of GTPase activity, whereas sanguinarine perturbs the Z ring but may be toxic as it targets mammalian cells [7].

Here we report the identification of FtsZ as one of the likely intracellular targets for antibacterial action of cinnamaldehyde. This phenylpropanoid compound binds FtsZ, inhibits the GTPase function and polymerization of *E. coli* FtsZ in the micro molar range and perturbs the Z-ring assembly *in vivo*, an assembly essential for bacterial cell division. Interestingly, it can offer equivalent bactericidal activities against both, the susceptible and multi drug resistant Gram-positive and Gram-negative pathogenic bacteria isolated from human subjects, with no development of any resistance even after 10 successive passages at sub-inhibitory concentrations [9], which implies its role as a successful inhibition of FtsZ inhibitor. It induces cell filamentation and disintegrates *E. coli* cytokinesis. Cinnamaldehyde is the only plant based small molecule inhibitor of FtsZ, whose binding epitopes for FtsZ are clearly identified for the first time in this study, along with a proposed binding site in the C terminal pocket of FtsZ involving the T7 loop.

In this study, the predominant form of cinnamaldehyde, i.e. *trans* isomer is used, although *cis* and *trans* isomers both exist. *Trans*-cinnamaldehyde, 3-phenyl-2-propenal, a potent aromatic compound isolated from the stem bark of *Cinnamomum cassia* is used in traditional medicine and pharmaceutical preparations for gastritis, cold, anti-aggregation of platelet, anti-mutagenic and bactericidal effects, e.g. Weitongding tablet (WTDT) is a new Chinese traditional patent medicine, and Dihuang Pill (GDHP) is a herbal medicinal preparation [10,11]. This natural product is considered to be a non-toxic and safe fragrance agent with no acute or chronic toxicity, no mutageneticity or genotoxicity and no carcinogenicity detected in bacterial, insect and mammalian studies [12]. It completely inhibits the growth of numerous pathogenic species (rods and cocci) such as *Staphylococcus*, *Micrococcus*, *Bacillus*, *Enterobacter*, *Helicobacter pylori*, *Mycobacterium smegmatis* [9,13,14]. Among human intestinal bacteria, growth-inhibiting activity of cinnamaldehyde was more pronounced in harmful bacteria like *Cl. perfringens* and *B. fragilis*, as compared to the beneficial bacteria like *bifidobacteria* and *L. acidophilus* [15]. Treatment of the exponential phase cells with cinnamaldehyde results in filamentation and strong inhibition of cell separation in *B. cereus*, where the formation of septa was observed to be initiated but not completed when treated with cinnamaldehyde [16]. The mechanism of inhibition of growth of microbial cells by cinnamaldehyde remains unclear.

Here, we have demonstrated for the first time that FtsZ may be one of the target proteins for cinnamaldehyde. We have also shown that cinnamaldehyde inhibited cytokinesis of *E. coli* by perturbing the cytokinetic Z-ring formation probably by inhibition of the assembly of FtsZ protofilaments. In addition, a 3D model for FtsZ–cinnamaldehyde complex has been proposed here. The combination of saturation transfer difference (STD) NMR measurements [17–19] and *in silico* molecular modeling using the program AutoDock [20] helped in identifying the epitopes of the cinnamaldehyde interacting with FtsZ at atomic resolution.

2. Material and methods

2.1. Reagents

GTP, MES, EDTA, β-mercaptoethanol, LB, Tris–HCl, KCl, $MgCl_2$, DMSO, $CaCl_2$, polymyxin B, mellitin were purchased from Sigma (St. Louis, MO). IPTG was purchased from Molecular Probes (Johnson City, OR). Cinnamaldehyde was obtained from Aldrich (Milwaukee, WI). Nickel resin was from Qiagen (Chatsworth, CA). SDS-PAGE chemicals were purchased from BioRad (Richmond, CA). Alamar Blue was obtained from Alamar Biosciences Inc (Sacramento, CA). All other chemicals were of analytical grade.

2.2. Antibacterial and hemolytic activity of cinnamaldehyde

Minimum inhibitory concentration and minimum bactericidal concentration of *trans*-cinnamaldehyde were determined for Gram-negative *E. coli* and Gram-positive *B. subtilis* using the colorimetric (alamarBlue™) micro dilution broth assay [21]. For MIC determination, 1000 mg/mL polymyxin B was used as the positive control and bacterial strains were obtained as clinical isolates. In addition, MIC of cinnamaldehyde was also determined for methicillin resistant *S. aureus* by broth micro dilution method using National Committee for Clinical Laboratory Standards [22].

Further, the toxicity of cinnamaldehyde to eukaryotic cells was tested by its ability to lyse human red blood cells, and results were compared with mellitin as a standard. Hemolytic activity was performed as described earlier [23] for which 1000 and 2000 μg/mL cinnamaldehyde was assayed in duplicate.

2.3. FtsZ wild type and FtsZ–GFP purification

FtsZ was purified from the transformed recombinant *E. coli* K-12 strain AG1 containing plasmid pCA24N with gene inset for untagged FtsZ (EcoGene accession no. EG10347) [24]. Cells grown in LB media were induced (0.5 mM IPTG), harvested, sonicated and purified on a Nickel–NTA Agarose resin column by eluting with 300 mM imidazole. Fractions were dialyzed with 50 mM Tris–HCl pH 8.0, 50 mM KCl, 10% glycerol, 1 mM EDTA by AKTA FPLC UPC–900 system (GE Healthcare Ltd, UK),

pooled, concentrated and analyzed by 12.5% SDS PAGE. Homogeneity of purified FtsZ was assessed by dynamic light-scattering measurements (DynaPro™ Protein Solutions, Santa Barbara, CA). FtsZ aliquots were stored at −80 °C.

2.4. Light-scattering assay for FtsZ polymerization and IC_{50} determination

A standard light-scattering assay [25] was used to determine whether cinnamaldehyde could inhibit GTP initiated *in vitro* polymerization of recombinant wild type *E. coli* FtsZ. In brief, untagged FtsZ (12.5 μM)) was polymerized in assembly buffer A (50 mM MES pH 6.5, 50 mM KCl, 5 mM $MgCl_2$, 1 mM GTP) in the presence of cinnamaldehyde (0–200 μM) and monitored in a LS 55 fluorescence spectrometer (Perkin-Elmer® Corp. MA).

2.5. GTP hydrolysis assay for FtsZ

A standard malachite green sodium molybdate assay [26] was employed to quantify the inorganic phosphate produced due to hydrolysis of GTP during FtsZ assembly in the presence of cinnamaldehyde (0–200 μM).

2.6. Electron microscopy of FtsZ protofilaments

Untagged-wild type control FtsZ, 12.5 μM was incubated in assembly buffer A for 10 min. 100 μM cinnamaldehyde was added to FtsZ protofilaments. After 5 min, the sample was placed on a carbon coated EM copper grid (300-mesh size) for 60 s, and then the grid was blotted dry and negatively stained with 2% phospho-tungstate for 45 s [27]. Images were collected using CM 200 transmission electron microscope (Philips Electron Optics, FEI Co. Hillsboro, Ore) at 50,000× magnification.

2.7. Spatial characteristics of Z-ring of E. coli cells in vivo

An overnight culture of *E. coli* cells expressing FtsZ–GFP-tagged was diluted 1:10 in fresh LB broth [28]. Pre-log phase cells (OD_{600} = 0.3) were treated with 100 μM cinnamaldehyde for 75 min and observed using LSM 510 META^{Mk4} laser scanning fluorescence microscope (Carl Zeiss Micro Imaging GmbH, Germany) at 100× oil magnification, standard fluorescein isothiocyanate filter set for GFP. Z-ring analysis was done using Image J (U.S. National Institutes of Health, Maryland, USA) and Image–Pro® software (Media Cybernetics, Silver Spring, MD). 100 cells were analyzed to calculate the frequency of FtsZ rings.

2.8. Isothermal titration calorimetry

ITC measurements were performed [29] on VP–ITC Micro-Calorimeter (MicroCal™ Inc, Northampton, MA). 0.01 mM FtsZ and 0.025 mM cinnamaldehyde were dialyzed against the same buffer (50 mM MES pH 6.8, 50 mM KCl, and 5 mM $MgCl_2$). A typical titration involved 50 injections of cinnamaldehyde (5 μL aliquots per shot) at 3 min intervals, into the sample cell (volume ~1.4 mL) containing FtsZ. The heat of dilution of ligand in the buffer alone was subtracted from the titration data. The data was analyzed using Origin® 5.0.

2.9. Saturation transfer difference (STD) NMR spectroscopy

The exchangeable protons of FtsZ were exchanged to deuterated buffer 50 mM sodium phosphate buffer, pH 6.5 (the pH value is uncorrected for the deuterium effects), 50 mM NaCl, 5 mM $MgCl_2$ by ultra filtration. All STD NMR experiments were performed on an AVANCE™ DRX-600 NMR spectrometer (Bruker BioSpin Pte Ltd.) equipped with a cryoprobe at 298 K using the WATERGATE 3-9-19 sequence for water suppression. Maximal STD effects can be obtained when it is performed at protein to ligand ratio of 1:100 [30]. 1D STD NMR spectra of 15 μM of FtsZ and 1500 μM of cinnamaldehyde (molar ratio 1:100) were recorded using the standard pulse sequence [17] with a 30-ms spin-lock pulse of 15 kHz. FtsZ was irradiated at 0.15 ppm (on-resonance) and at 40 ppm (off-resonance), where no NMR resonances are present. Subtraction of the two spectra by phase cycling led to a differential spectrum containing the signal from the saturation transfer. 256 scans were used for the reference spectra and 512 for the difference spectra. Spectrum of cinnamaldehyde was assigned under the same conditions as the STD NMR spectra. Data processing was performed using the TopSpin® program suite (Bruker BioSpin Pte Ltd.). For group epitope mapping analysis of cinnamaldehyde, relative STD values for the protons were calculated by arbitrarily assigning a value of 100% to the most intense STD signal.

2.10. In silico molecular modeling

AutoDock 3.0 [20] was employed to dock the PDB coordinates of the cinnamaldehyde (http://chemistry.gsu.edu) into *E. coli* FtsZ homology model, built from the X–ray crystal structure of *M. jannaschii* (PDB:1FSZ, 2.8 Å) [31] template using Insight II® 2005 (Accelrys, CA, USA). SYBYL 7.1 (Tripos Inc., St. Louis, MO) was employed to assign the Kollmann all atom charges prior to docking. Grid maps were constructed using 127 × 127 × 127 points, with grid spacing of 0.375 Å. 250 Lamarckian genetic algorithm runs were performed and the maximum number of accepted and rejected trials per cycle was set to 10^6. Binding modes were clustered using an r.m.s deviation cut-off of 1.0 Å with respect to the starting position.

3. Results

3.1. Antibacterial and hemolytic activity of cinnamaldehyde

Cinnamaldehyde exhibited a broad spectrum of antibacterial activity against antibiotic sensitive and resistant bacteria. Minimum inhibitory concentration (MIC) of cinnamaldehyde against *E. coli* and *B. subtilis* were determined to be 1000 and 500 mg/L, respectively (data not presented). For concentrations less than MIC, aerobic microbiological activity caused alamarBlue™ redox dye to change from blue to pink. For methicillin resistant *Staphylococcus aureus* strain (MRSA), the broth dilution method showed an MIC of 250 mg/L. MIC of cinnamaldehyde for MRSA was the same as reported earlier [32]. MIC endpoint was read as the lowest concentration of cinnamaldehyde *in vivo* at which no visible growth was

observed for *E. coli*, *B. subtilis* and MRSA. Cinnamaldehyde showed a minimum bactericidal concentration (MBC) of 1000 mg/L against both *E. coli* and *B. subtilis*, respectively. The MBC was the lowest concentration of cinnamaldehyde that killed 99.9% of the original inoculum of *E. coli* and *B. subtilis* in 48 h and more.

In the experiment used to evaluate cytotoxicity for red blood cells, positive control mellitin showed strong hemolytic activity with 100% lysis after 60 min. However, the highest concentrations of cinnamaldehyde tested (1000 and 2000 μg/L) showed 0% hemolysis. Thus, even at doses higher than its minimum inhibitory and minimum bactericidal concentrations, cinnamaldehyde showed no hemolytic activity for human erythrocytes.

3.2. *Cinnamaldehyde inhibits FtsZ assembly*

Cinnamaldehyde strongly inhibited the light-scattering signal of FtsZ assembly. The decrease in light-scattering intensity of the FtsZ assembly in the presence of cinnamaldehyde indicates the decrease in the polymer mass of FtsZ protofilaments. Fig. 1 shows the effect of cinnamaldehyde on the kinetics of FtsZ assembly *in vitro*. GTP-dependent FtsZ polymerization is inhibited by cinnamaldehyde in a concentration dependent manner. IC_{50} of cinnamaldehyde for FtsZ was found to be 6.86 ± 2.2 μM ($n = 5$). Since the assembly of FtsZ protofilaments is dependent on GTPase activity, it was important to investigate the effect of cinnamaldehyde on the hydrolysis of GTP. Cinnamaldehyde showed inhibition of FtsZ GTPase activity in a dose dependent manner with an IC_{50} of 5.81 ± 2.2 μM (Fig. 2).

Electron microscopic images showed the visual evidence for the inhibition of wild type FtsZ protofilaments in the presence of cinnamaldehyde. In the absence of cinnamaldehyde, a dense network of GTP induced FtsZ protofilaments was

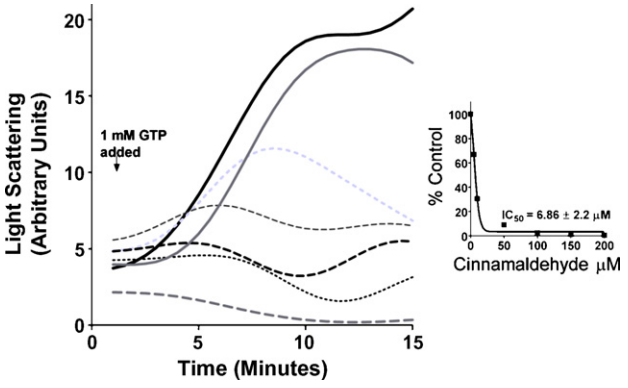

Fig. 1 – Effect of cinnamaldehyde on FtsZ assembly *in vitro*. The polymerization of GTP induced FtsZ was monitored as a function of light scattering in following concentrations of cinnamaldehyde, 0 μM (——), 5 μM (——), 10 μM (·····), 50 μM (——), 100 μM (- - -), 150 μM (···), 200 μM (——). The % control activity of various cinnamaldehyde concentrations (Inset) was calculated by comparison with an assay without cinnamaldehyde and IC_{50} value of 6.86 ± 2.2 μM was obtained. The experiment was performed in triplicate and average spectra are shown.

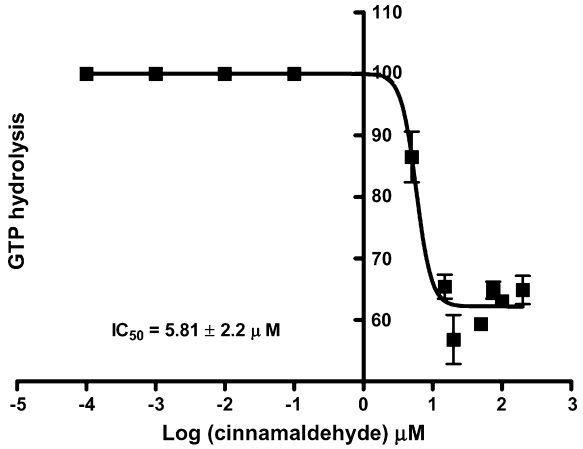

Fig. 2 – Effect of cinnamaldehyde on the GTPase activity of FtsZ. GTP hydrolysis was carried out in the presence of cinnamaldehyde (0–200 μM) by adding 1 mM GTP. IC_{50} of 5.81 ± 2.2 μM was observed in presence of cinnamaldehyde. The experiment was done for three times.

observed, shown by dark arrows (Fig. 3A). Cinnamaldehyde inhibited the *in vitro* bundling of FtsZ protofilaments in a dose-dependent manner. In presence of 100 μM cinnamaldehyde, except for a few straight, thin filaments, complete inhibition of polymerization was observed, as shown in Fig. 3B. Since light-scattering data showed almost 80% inhibition of FtsZ polymerization for 100 μM cinnamaldehyde, it was chosen as the test concentration for imaging studies in this study.

3.3. *Cinnamaldehyde targets Z-ring characteristics in vivo*

Confocal imaging of live *E. coli* cells with GFP tagged FtsZ was done under 100 μM concentration of cinnamaldehyde. In the absence of cinnamaldehyde, the normal pattern of FtsZ localization with bands of FtsZ-tagged GFP fluorescence (seen as Z-ring pattern) was observed at the mid-cell (Fig. 4A). Treatment with 100 μM cinnamaldehyde perturbed the Z-ring morphology (Fig. 4B). Addition of cinnamaldehyde resulted in a reduction of Z-rings from 85.7% (0 μM) to 58% (100 μM) along with a reduction in frequency of Z-ring per unit cell length of *E. coli* from 5.00 to 2.88. Fig. 4B shows cell elongation induced by 100 μM cinnamaldehyde. The mean length of 3.4 μm in control *E. coli* cells can be compared with mean length of 7.2 μm in treated cells.

3.4. *Cinnamaldehyde binds to FtsZ*

The interactions between FtsZ and cinnamaldehyde were studied by the isothermal titration calorimetry (Fig. 5). The initial injection of cinnamaldehyde into FtsZ resulted in binding of cinnamaldehyde and generation of maximal heat associated with the total enthalpy of the interaction. With subsequent injections, the amount of FtsZ available for binding decreased. A concomitant reduction in complex formation led to reduction of associated heat of interaction. Eventually all the FtsZ was found in the complex and no further heat of binding was observed (Fig. 5A). The heats of

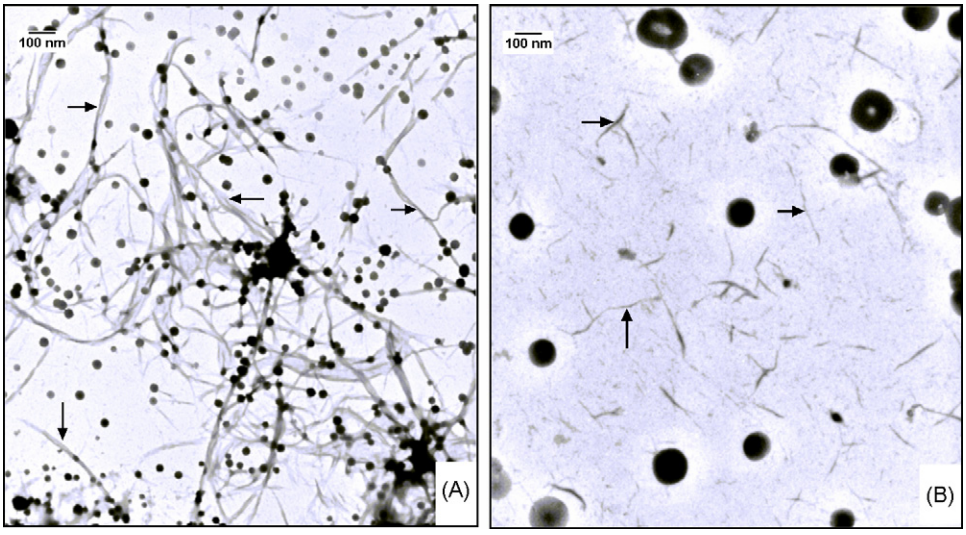

Fig. 3 – Inhibitory effect of cinnamaldehyde on preformed FtsZ wild type protofilaments by electron microscopy. Electron micrograph (A) illustrated the polymerized network of FtsZ (12.5 μM) upon addition of 1 mM GTP in 50 mM MES pH 6.8, 50 mM KCl, 5 mM $MgCl_2$ buffer. The dark arrows are pointed to show the protofilaments (B) illustrated the loss of polymerized FtsZ bundles (this is shown by the dark arrows) when treated with 100 μM cinnamaldehyde. The grid was searched thoroughly to trace a few sections containing dot like FtsZ structures, as seen in (B). The scale bar is 100 nm.

individual injections were integrated with respect to time and plotted against molar ratio of cinnamaldehyde (Fig. 5B). When the resultant titration curve was fitted using one site binding model, it yielded an association constant of $1.0 \times 10^6 \pm 0.2\ M^{-1}$ and enthalpy change (ΔH) of -11.260 ± 6.150 Kcal $mole^{-1}$ for a binding stoichiometry of $n = 1$. The free energy (ΔG) and the entropy (ΔS) calculated were -8.16 Kcal $mole^{-1}$ and -0.0106 Kcal $mole^{-1}$ deg^{-1}, respectively.

3.5. *Epitope mapping of cinnamaldehyde*

To determine the pharmacophoric groups of cinnamaldehyde bound to FtsZ, 1D STD NMR spectroscopy [17–19] was performed. The STD NMR spectroscopy detected the magnetization that was transferred from FtsZ to the bound cinnamaldehyde protons. It further confirmed the binding of cinnamaldehyde to FtsZ as only bound ligands show STD effects. 1D STD NMR spectrum of the FtsZ–cinnamaldehyde complex is shown in Fig. 6. The relative STD values of the individual protons were obtained from the reference and STD spectra, respectively, (Fig. 6A and B). The difference spectrum (Fig. 6B) contained only signals of cinnamaldehyde, with low molecular weight impurities being removed. Fig. 6C reflects the relative amount of saturation exclusively transferred to cinnamaldehyde which bound to FtsZ. It was found that the H2 and H3 of the conjugated alkene of cinnamaldehyde

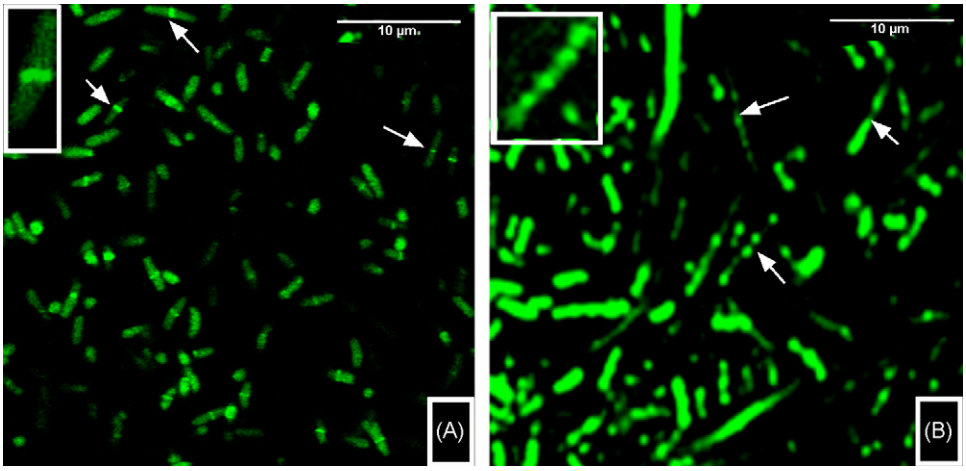

Fig. 4 – Effect of cinnamaldehyde on Z-ring spatial characteristics by confocal microscopy. (A) and (B) show a typical result for *E. coli* cells bearing an FtsZ-GFP fusion. Shown are control cells with typical Z ring pattern, as shown by arrows (A), cells treated with 100 μM cinnamaldehyde show elongation in cell length with dissipated Z-ring morphology, as indicated by arrows (B). Insets in both panels show an enlarged view of an individual *E. coli* cell. Cinnamaldehyde reduced the frequency of Z-ring occurrence/unit cell length in *E. coli* bacteria and perturbed the Z-ring morphology. The scale bar is 10 μm.

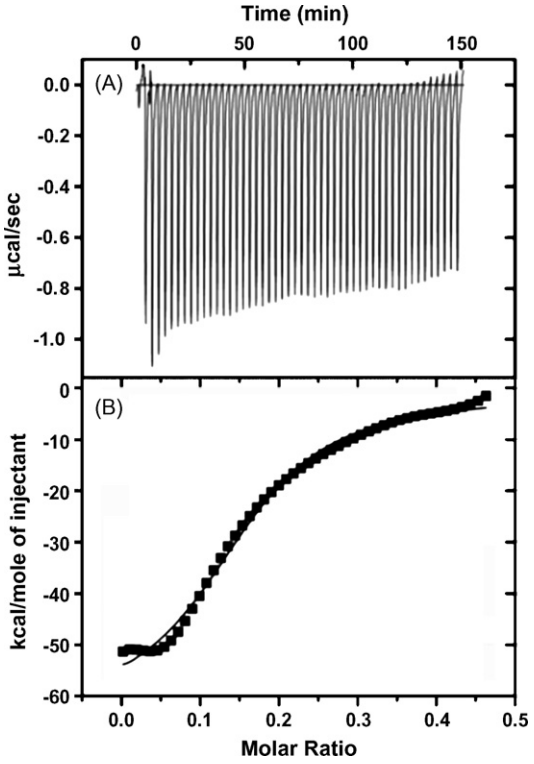

Fig. 5 – Thermodynamic characterization of FtsZ–cinnamaldehyde interaction by ITC. (A) Titration of 10.0 μM FtsZ with 25 μM cinnamaldehyde (5 μL injection steps) in 50 mM MES, 50 mM KCl, 10 mM $MgCl_2$ pH 6.8 at 20 °C, as raw data. The rate of heat released is plotted as a function of time. (B) Plot of heat of exchange per mole of cinnamaldehyde vs. molar ratio of FtsZ after subtraction of buffer control.

received the largest relative saturation transfer of 94% and 100%, respectively (Fig. 6C), and therefore, are most intimately bound to FtsZ. All the protons of the aromatic ring showed medium STD response of around 70% (Fig. 6C), suggesting that these protons have less intimate contacts with the FtsZ surface in comparison to the H2 or H3. However, H1 was an exchangeable proton and it was exchanged with the D_2O buffer.

3.6. *Molecular modeling*

In silico molecular modeling was performed using AutoDock program which gave a docking model built from the flexible conformational space of cinnamaldehyde, assuming the FtsZ receptor to be rigid. Auto Docking resulted into one major (210 conformations) and one minor cluster (40 conformations). The conformation of minor cluster showed that H2 and H3 are close to the FtsZ surface but the aromatic ring was pointing towards the solution and hence was ruled out. The lowest energy conformation from the major cluster of AutoDock was considered as it was in agreement with the results obtained from STD NMR spectroscopy. The close view of the putative binding pocket involved in FtsZ–cinnamaldehyde interaction is shown in Fig. 7 using PyMOL. This model predicted a strong possibility of interaction between H2 of cinnamaldehyde and G295 (~2.2 Å) of FtsZ; and between H3 of cinnamaldehyde and methyl group of V208 (~1.8 Å). Interestingly, these residues are conserved among FtsZ from several species. In the docking model (Fig. 7), the aromatic ring of cinnamaldehyde was near the aliphatic-side chains of P203, M206, N207 and V208 of T7-loop of FtsZ, whereas the carbonyl group of cinnamaldehyde was found in close proximity to the side chain amino group of N263 (~1.8 Å), guanidinium group of R202 (~3.8 Å) and hydroxyl group of S297 (~2.8 Å). These findings on group epitope mapping agreed well with the docked conformation of

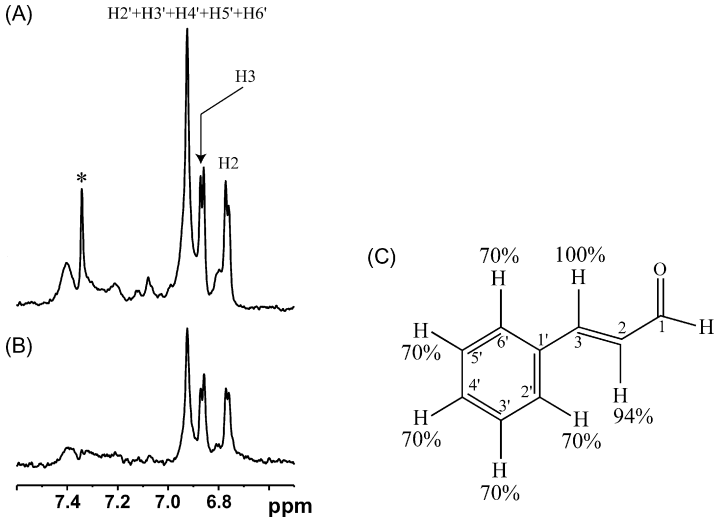

Fig. 6 – Group epitope mapping of cinnamaldehyde bound to FtsZ. (A) Reference 1D NMR spectrum of cinnamaldehyde–FtsZ complex at 298 K and 600 MHz, using a 30-ms spin-lock pulse of 30 dB is shown. Asterisk indicates the signal for impurities in the buffer. (B) Corresponding STD NMR spectrum showing that cinnamaldehyde yields signals and therefore binds to FtsZ. The impurity did not bind to FtsZ, as this signal is absent in the STD spectrum. (C) Structure of cinnamaldehyde and the relative degrees of saturation of individual protons normalized to that of the H3 proton, as determined from 1D STD NMR spectra, are shown. Higher % indicates a closer proximity to the FtsZ surface.

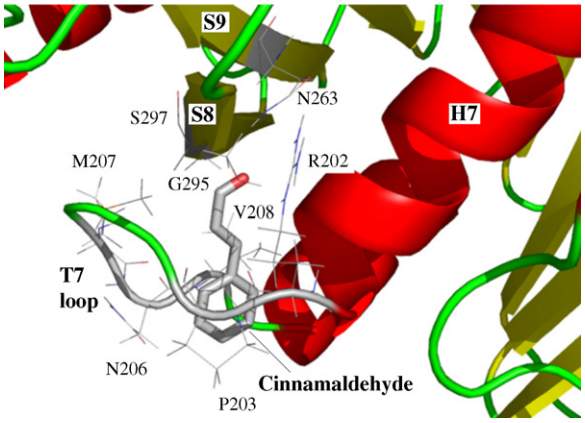

Fig. 7 – Putative binding pocket for cinnamaldehyde in *E. coli* FtsZ. Close view of AutoDock model for cinnamaldehyde–FtsZ interaction is shown, involving the T7 loop binding pocket. For simplicity hydrogens of cinnamaldehyde are omitted. The labeled residues of FtsZ involved in binding with cinnamaldehyde can be compared to the STD NMR data. In FtsZ, H7, S8, S9 stands for central helix 7, and β sheets 8 and 9, respectively.

cinnamaldehyde. In the proposed model, the binding of cinnamaldehyde to FtsZ involves the T7 loop pocket, similar to SulA, another known FtsZ inhibitor that binds to the T7 loop.

4. Discussion

Considerable efforts have been made to identify antibacterial drugs that target the cell division protein FtsZ in an attempt to establish novel drugs with a unique mode of action. Here, we have shown that cinnamaldehyde binds FtsZ, inhibits its assembly and perturbs the formation of the Z-ring, thus inhibiting the process of cell division.

In vitro, the inhibition of FtsZ by cinnamaldehyde was confirmed by the reduction in light scattering of polymerized FtsZ and inhibition of FtsZ polymers was visualized by electron microscopy. Further, cinnamaldehyde was also found to be a potent inhibitor of the GTPase activity of FtsZ that explains its ability to depolymerize preformed FtsZ polymers. The results of confocal microscopy of live *E. coli* cells showed that cinnamaldehyde specifically targeted Z ring spatial arrangement by dissipating the Z-rings and reducing frequency of Z-ring formation per unit cell length of *E. coli* to almost half. Cinnamaldehyde increased the average cell length of *E. coli* and perturbed Z-ring morphology by depletion of FtsZ protofilaments. This further justifies its inhibitory effect on cell division via FtsZ as a target, because cinnamaldehyde is also known to significantly decrease the exponential growth rate in *Bacillus cereus* [33] and specific growth rate in *E. coli* ATCC 33456, *Pseudomonas* strains in a dose dependent manner [34]. The frequency of Z-ring formation in normal cell division is also proportional to growth rate of bacteria [35]. As reported earlier, cinnamaldehyde does not disintegrate the outer membrane or deplete the intracellular ATP pools in bacteria [36], suggesting that cinnamaldehyde could gain access to the periplasm and to the deeper parts of the cell, probably through the outer membrane traversing porins [37]. Thus, one of the modes of antibacterial activity of cinnamaldehyde may be attributed to perturbation of Z-rings and inhibition of cytokinesis.

Cinnamaldehyde can be generally considered a bactericidal compound as it has an MBC almost equal to its MIC for *E. coli* and *B. subtilis*. In this study, the MIC of cinnamaldehyde against MRSA is 250 μg/mL which correlates with the earlier report [32]. The acrolein group in the cinnamaldehyde has been elucidated to be an essential element for the antibacterial activity [38]. But when exposed to air, the reactive unsaturated aldehyde would readily oxidize *trans*-cinnamaldehyde to cinnamic acid [39]. This would cause volatile loss and instability of *trans*-cinnamaldehyde and *in vivo*, it might decompose prior to carrying out its bactericidal activity. This would result in varying range of MIC's of *trans*-cinnamaldehyde for a bacterial strain, e.g. here the MIC of *trans*-cinnamaldehyde in *E. coli* is 1000 μg/mL. Although some reports suggest MIC to be in the range of 75–600 μg/mL [40,32], it has also been reported to be merely 1 μg/mL [9]. But since cinnamaldehyde inhibits MRSA and other antibiotic-resistant strains of *M. tuberculosis*, *Escherichia*, *Enterococcus and Staphylococcus* [9], it can serve as a template for developing a novel class of antimicrobial compounds to combat continuous emergence of antibiotic resistance by targeting FtsZ. Cinnamaldehyde displayed potent broad spectrum antibacterial activity but no significant hemolytic activity, indicating that it may be good lead to develop new drugs against bacterial infections. Moreover, a nearly linear relationship between antibacterial activity (MIC for *E. coli*) and *E. coli* FtsZ inhibition (IC_{50}) was observed. This infers [41] that FtsZ can be a selective mode of action for the cinnamaldehyde and a more therapeutic effect rather than a toxic effect is exerted by cinnamaldehyde.

It is known that cinnamaldehyde is a reactive aldehyde due to the α,β-unsaturated carbonyl moiety in its side chain. *In vivo*, large quantities of the absorbed cinnamaldehyde can be rapidly and irreversibly oxidized to cinnamic acid by enzymatic catalysis, making it unstable in blood [42]. However, micro encapsulation of *trans*-cinnamaldehyde for administration *in vivo* could help in preventing this degradation. A recent report on micro encapsulation of cinnamon oleoresin by spray drying using binary and ternary blends of gum arabic, malto-dextrin, and modified starch could successfully stabilize and protect the degradation of cinnamaldehyde, its major (90%) constituent from light, oxygen and volatile loss [43]. Although micro encapsulation is already a widely accepted drug delivery method that allows longer-lasting half-lives of drugs, sustained/controlled release, drug site targeting and reduced toxicity, further studies are clearly required for evaluating the stability and overall efficacy of encapsulated cinnamaldehyde *in vivo*. Nevertheless, other novel approaches are being successfully attempted to develop administration of cinnamaldehyde *in vivo*. Recently, in mice, a direct delivery route via the intranasal inoculation and inhalation of vapor was found to be an effective and safe delivery route for cinnamaldehyde in improving lethal influenza [44].

Binding of cinnamaldehyde to FtsZ was characterized by ITC and 1D STD NMR experiments. Isothermal calorimetric

titration revealed an exothermic and thermodynamically driven FtsZ–cinnamaldehyde interaction with an association constant of $1.0 \pm 0.2\ \mu M^{-1}$. Release of heat occurred as FtsZ went from free (unbound) to the bound state. Since ΔH is negative, i.e. -11.260 ± 6.150 kcal/mole, a favorable enthalpic interaction [45] indicated a high affinity of cinnamaldehyde for its FtsZ binding site. A negative binding free energy, i.e. −8.16 kcal/mol, confirmed a favorable interaction between cinnamaldehyde and FtsZ [46]. The dissociation constant indirectly obtained from ITC results was observed to be one order of magnitude lower than IC_{50} for FtsZ inhibition and fairly consistent to fit the standard Cheng Prusoff equation [47] for functional binding assay. The binding of cinnamaldehyde to FtsZ was also confirmed by fluorescence spectroscopy which showed an 800-fold enhancement in cinnamaldehyde fluorescence along with a significant 20 nm blue shift from 327 to 307 nm (data not shown) as cinnamaldehyde bound to FtsZ.

STD NMR experiments in conjunction with AutoDock model gave precise information about the binding epitope of cinnamaldehyde, which is important for the design of a potent drug. The experimentally determined STD effects clearly identified H2 and H3 protons (94% and 100%, respectively) of conjugated alkene of cinnamaldehyde to be in close contact with FtsZ protons in the binding pocket of FtsZ. The AutoDock model showed that H2 proton is in close vicinity to G295 and the H3 proton is near to the methyl group of hydrophobic V208 of FtsZ. All the aromatic protons of the cinnamaldehyde also gave medium STD response (70%), indicating that the aromatic ring was also necessary for the binding. Conjugated alkene and aromatic ring of cinnamaldehyde are its planar functional groups which may interact with the binding pocket of FtsZ by means of Van der Waals or hydrophobic interactions.

Further, H1 of cinnamaldehyde being an exchangeable proton, no STD NMR assignments were possible for it. Earlier reports have suggested that the carbonyl group of cinnamaldehyde was involved in binding with proteins [48]. The cinnamaldehyde binding site on other proteins involved cysteine [49], serine [50], and asparagine and glutamine residues [51]. Here, the docking model suggested that the carbonyl group of cinnamaldehyde is in close proximity of side chain amino group of N263, guanidinium of R202 and hydroxyl group of S297. This indicates that cinnamaldehyde may interact with FtsZ through hydrogen bonds as well. Interestingly, multiple sequence alignment analysis revealed that G295, V208, R202, N263 and S297 are found to be highly conserved among the FtsZ. Hence, it can be speculated that the interaction of these conserved residues with cinnamaldehyde could be a common feature for FtsZ from several species.

In addition, N263 and S297 are three dimensionally close to the T7 loop of FtsZ, whereas the position of R202 and V208 is in the T7 loop itself. Binding of cinnamaldehyde to these residues would probably result in perturbation of the conformation of the T7 loop, which is involved in the GTPase activity of the FtsZ [52]. Our experiments have shown that cinnamaldehyde inhibits GTPase activity of FtsZ, further corroborating the above proposition. Interestingly, crystal structure of the SOS-inducible cell division inhibitor SulA in complex with FtsZ from *Pseudomonas aeruginosa* revealed that SulA binds to the T7 loop surface of FtsZ [53]. Like cinnamaldehyde, SulA also inhibits GTPase activity and affects FtsZ polymerization, revealing an effective evolutionary strategy for targeting FtsZ. From the sequence alignment, we found that residues that bind SulA are also adjacent to the residues of FtsZ proposed to be involved in cinnamaldehyde binding, especially V208, R202, and N263 and G295. Based on this observation, we performed a competitive binding experiment of SulA and cinnamaldehyde with FtsZ. Our preliminary data showed a possibility of an overlap of SulA and cinnamaldehyde binding pocket (data not shown). This further strengthens the reliability of our FtsZ–cinnamaldehyde complex model.

Hence, our finding that a small molecule inhibitor like cinnamaldehyde binds around the T7 loop may be significant to further predict a novel class of destabilizing anti-FtsZ agents. These compounds may bind to the T7 loop in one FtsZ monomer inducing such conformational changes that one FtsZ monomer fails to make optimum contact with the GTP binding T1–T6 loop in the neighboring monomer and thereby inhibits FtsZ polymerization. The results reported here have confirmed that cinnamaldehyde inhibits bacterial cell division protein FtsZ. This work suggests that although cinnamaldehyde is unstable it could be considered a new source for antibacterial drug development. Since its pharmacophoric groups have been identified here, it could be a lead structure for the design of more stable and potent anti-FtsZ agents as well as a vital tool for understanding the regulatory role of FtsZ in cell division.

Acknowledgements

We thank Prof. H Mori, Nara Institute of Science and Technology, Japan for the FtsZ clone. We thank the Dept. of Microbiology, PD Hinduja Hospital, Mumbai for providing MRSA strain and Dr R Kelkar, Tata Memorial Centre, Mumbai for MIC strains. J.S and S.S acknowledge the research grant support from the Academic Research Fund, National University of Singapore (NUS). We thank EM facilities at the Dept. of Biological Sciences, NUS and Temasek Life Science Laboratories, Singapore for confocal microscopy work. We thank Dr S Bhattacharjya, Nanyang Technological University, Singapore for NMR spectrometer and RaviPrakash Reddy for modeling study. Lastly, DD acknowledges Department of Atomic Energy Grant No. 37/47/BRNS/2291.

REFERENCES

[1] Vollmer W. The prokaryotic cytoskeleton: a putative target for inhibitors and antibiotics? Appl Microbiol Biotechnol 2006;73:37–47.
[2] Bi EF, Lutkenhaus J. FtsZ ring structure associated with division in *Escherichia coli*. Nature 1991;354:161–4.
[3] RayChaudhuri D, Scott GG, Wright A. How does a bacterium find its middle? Nat Struct Biol 2000;7:997–9.
[4] Wang J, Galgoci A, Kodali S, Herath KB, Jayasuriya H, Dorso K, et al. Discovery of a small molecule that inhibits cell division by blocking FtsZ, a novel therapeutic target of antibiotics. J Biol Chem 2003;278:44424–8.

[5] Urgaonkar S, La Pierre HS, Meir I, Lund H, RayChaudhuri D, Shaw JT. Synthesis of antimicrobial natural products targeting FtsZ: (+/−)-dichamanetin and (+/−)-2′ ″-hydroxy-5′ ′-benzylisouvarinol-B. Org Lett 2005;7:5609–12.
[6] Margalit DN, Romberg L, Mets RB, Hebert AM, Mitchison TJ, Kirschner MW, et al. Targeting cell division: small-molecule inhibitors of FtsZ GTPase perturb cytokinetic ring assembly and induce bacterial lethality. Proc Natl Acad Sci USA 2004;101:11821–6.
[7] Beuria TK, Santra MK, Panda D. Sanguinarine blocks cytokinesis in bacteria by inhibiting FtsZ assembly and bundling. Biochemistry 2005;44:16584–93.
[8] Ito H, Ura A, Oyamada Y, Tanitame A, Yoshida H, Yamada S, et al. A 4-aminofurazan derivative – A189 – inhibits assembly of bacterial cell division protein FtsZ *in vitro* and *in vivo*. Microbiol Immunol 2006;50:759–64.
[9] Ali SM, Khan AA, Ahmed I, Musaddiq M, Ahmed KS, Polasa H, et al. Antimicrobial activities of eugenol and cinnamaldehyde against the human gastric pathogen *Helicobacter pylori*. Ann Clin Microbiol Antimicrob 2005;4:20.
[10] Yu BS, Lai SG, Tan QL. Simultaneous determination of cinnamaldehyde, eugenol and paeonol in traditional Chinese medicinal preparations by capillary GC-FID. Chem Pharm Bull 2006;54:114–6.
[11] Yanaga A, Goto H, Nakagawa T, Hikiami H, Shibahara N, Shimada Y. Cinnamaldehyde induces endothelium-dependent and -independent vasorelaxant action on isolated rat aorta. Biol Pharm Bull 2006;29:2415–8.
[12] Bickers D, Calow P, Greim H, Hanifin JM, Rogers AE, Saurat JH, et al. A toxologic and dermatologic assessment of cinnamyl alcohol, cinnamaldehyde and cinnamic acid when used as fragrance ingredients. The RIFM expert panel. Food Chem Toxicol 2005;43:799–836.
[13] Masuda S, Hara-Kudo Y, Kumagai S. Reduction of *Escherichia coli* O157:H7 populations in soy sauce, a fermented seasoning. J Food Prot 1998;61:657–61.
[14] Moleyar V, Narasimham P. Antibacterial activity of essential oil components. Int J Food Microbiol 1992;16: 337–42.
[15] Lee HS, Ahn YJ. Growth-inhibiting effects of *Cinnamomum cassia* bark-derived materials on human intestinal bacteria. J Agric Food Chem 1998;46:8–12.
[16] Kwon JA, Yu CB, Park HD. Bacteriocidal effects and inhibition of cell separation of cinnamic aldehyde on *Bacillus cereus*. Lett Appl Microbiol 2003;37:61–5.
[17] Mayer M, Meyer B. Characterization of ligand binding by saturation transfer difference NMR spectroscopy. Angew Chem Int Ed 1999;38:1784–8.
[18] Meyer B, Peters T. NMR spectroscopy techniques for screening and identifying ligand binding to protein receptors. Angew Chem Int Ed 2003;42:864–90.
[19] Bhunia A, Jayalakshmi V, Benie AJ, Schuster O, Kelm S, Ramakrishna N, et al. Saturation transfer difference NMR and computational modelling of a sialoadhesin–sialyl lactose complex. Carbohydr Res 2004;339:259–67.
[20] Morris GM, Goodsell DS, Halliday RS, Huey R, Hart WE, Belew RK, et al. Automated docking using a Lamarckian genetic algorithm and empirical binding free energy function. J Comp Chem 1998;19:1639–62.
[21] Collins LA, Franzblau SG. Microplate Alamar Blue assay versus BACTEC 460 system, for high-throughput screening of compounds against *Mycobacterium tuberculosis* and *Mycobacterium avium*. Antimicrob Agents Chemother 1997;41:1004–9.
[22] National Committee for Clinical Laboratory Standards. Methods for dilution antimicrobial susceptibility tests for bacteria that grow aerobically, fourth edition: approved standard, M7-A4. Villanova, Pennsylvania: National Committee for Clinical Laboratory Standards, 1997.
[23] Ferre R, Badosa E, Feliu L, Planas M, Montesinos E, Bardaji E. Inhibition of plant-pathogenic bacteria by short synthetic cecropin A-melittin hybrid peptides. Appl Environ Microbiol 2006;72:3302–8.
[24] Kitagawa M, Ara T, Arifuzzaman M, Nakamichi T, Inamoto E, Toyonaga H, et al. Complete set of ORF clones of *Escherichia coli* ASKA library (A Complete Set of *E. coli* K-12 ORF Archive): unique resources for biological research. DNA Res 2005;12:291–9.
[25] Mukherjee A, Lutkenhaus J. Analysis of FtsZ assembly by light scattering and determination of the role of divalent metal cations. J Bacteriol 1999;181:823–32.
[26] Geladopoulos TP, Sotiroudis TG, Evangelopoulos AE. A malachite green colorimetric assay for protein phosphatase activity. Anal Biochem 1991;192:112–6.
[27] Santra MK, Dasgupta D, Panda D. Deuterium oxide promotes assembly and bundling of FtsZ protofilaments. Proteins 2005;61:1101–10.
[28] Yu XC, Margolin W. Ca^{2+} mediated GTP-dependent dynamic assembly of bacterial cell division protein FtsZ into asters and polymer networks *in vitro*. EMBO J 1997;16:5455–63.
[29] Gupta S, Chakraborty S, Poddar A, Sarkar N, Das KP, Bhattacharyya B. Bis-ANS binding to tubulin: isothermal titration calorimetry the site-specific proteolysis reveal the GTP-induced structural stability of tubulin. Proteins 2003;50:283–9.
[30] Haselhorst T, Wilson JC, Thomson RJ, McAtamney S, Menting JG, Coppel RL, et al. Saturation transfer difference (STD) 1H-NMR experiments and *in silico* docking experiments to probe the binding of *N*-acetylneuraminic acid and derivatives to *Vibrio cholerae* sialidase. Proteins 2004;56:346–53.
[31] Lowe J, Amos LA. Crystal structure of the bacterial cell-division protein FtsZ. Nature 1998;391:203–6.
[32] Chang ST, Chen PF, Chang SC. Antibacterial activity of leaf essential oils and their constituents from *Cinnamomum osmophloeum*. J Ethnopharmacol 2001;77:123–7.
[33] Valero M, Giner MJ. Effects of antimicrobial components of essential oils on growth of *Bacillus cereus* INRA L2104 in and the sensory qualities of carrot broth. Int J Food Microbiol 2006;106:90–4.
[34] Niu C, Gilbert ES. Colorimetric method for identifying plant essential oil components that affect biofilm formation and structure. Appl Environ Microbiol 2004;70:6951–6.
[35] Weart RB, Levin PA. Growth rate-dependent regulation of medial FtsZ ring formation. J Bacteriol 2003;185: 2826–34.
[36] Helander IM, Alakomi HL, Latva-Kala K, Mattila-Sandholm T, Pol I, Smid EJ, et al. Characterization of the action of selected essential oil components on gram-negative bacteria. J Agric Food Chem 1998;46:3590–5.
[37] Nikaido H. Prevention of drug access to bacterial targets: permeability barriers and active efflux. Science 1994;264:382–8.
[38] Bae KH, Ji JM, Park KL. The antibacterial component from Cinnamomi cortex against a cariogenic bacterium *Streptococcus mutans* OMZ 176. Arch Pharm Res 1992;15: 239–41.
[39] Smith CK, Moore CA, Elahi EN, Smart AT, Hotchkiss SA. Human skin absorption and metabolism of the contact allergens, cinnamic aldehyde and cinnamic alcohol. Toxicol Appl Pharmacol 2000;168:189–99.
[40] Ooi LS, Li Y, Kam SL, Wang H, Wong EY, Ooi VE. Antimicrobial activities of cinnamon oil and cinnamaldehyde from the Chinese medicinal herb *Cinnamomum cassia* Blume. Am J Chin Med 2006;34:511–22.
[41] Barrett JF, Goldschmidt RM, Lawrence LE, Foleno B, Chen R, Demers JP, et al. Antibacterial agents that inhibit

two-component signal transduction systems. Proc Natl Acad Sci USA 1998;95:5317–22.
[42] Yuan JH, Dieter MP, Bucher JR, Jameson CW. Toxicokinetics of cinnamaldehyde in F344 rats. Food Chem Toxicol 1992;30:997–1004.
[43] Vaidya S, Bhosale R, Singhal RS. Microencapsulation of Cinnamon Oleoresin by spray drying using different wall materials. Drying Technol 2006;24:983–92.
[44] Hayashi K, Imanishi N, Kashiwayama Y, Kawano A, Terasawa K, Shimada Y, et al. Inhibitory effect of cinnamaldehyde, derived from Cinnamomi cortex, on the growth of influenza A/PR/8 virus *in vitro* and *in vivo*. Antiviral Res 2007;74:1–8.
[45] Luque I, Freire E. Structural parameterization of the binding enthalpy of small ligands. Proteins 2002;49:181–90.
[46] Moll D, Zimmermann B, Gesellchen F, Herberg FW. ITC in drug design. In: Hamacher M, Marcus K, Stühler K, Hall A, Warscheid B, Meyer HE, editors. Proteomics in drug research. New York: Wiley-Liss; 2006. p. 163–4.
[47] Cheng Y, Prusoff WH. Relationship between the inhibition constant (K1) and the concentration of inhibitor which causes 50 per cent inhibition (I50) of an enzymatic reaction. Biochem Pharmacol 1973;22:3099–108.
[48] Wendakoon CN, Sakaguchi M. Inhibition of amino acid decarboxylase activity of *Enterobacter aerogenes* by active components in spices. J Food Prot 1995;58:280–3.
[49] Weibel H, Hansen J. Interaction of cinnamaldehyde (a sensitizer in fragrance) with protein. Cont Dermatitis 1989;20:161–6.
[50] ShultZ RM, Cheerva AC. The binding of non specific transition state analogue to alpha chymotrypsin. FEBS Lett 1975;50:47–9.
[51] Shimoni L, Glusker JP. The geometry of intermolecular interactions in some crystalline fluorine-containing organic compounds. Struct Chem 1994;5:383–97.
[52] Scheffers DJ, de Wit JG, den Blaauwen T, Driessen AJ. GTP hydrolysis of cell division protein FtsZ: evidence that the active site is formed by the association of monomers. Biochemistry 2002;41:521–9.
[53] Cordell SC, Robinson EJH, Lowe J. Crystal structure of the SOS cell division inhibitor SulA and in complex with FtsZ. Proc Natl Acad Sci USA 2003;100:7889–94.